ELSEVIER

Journal of Nuclear Materials 296 (2001) 34–42

journal of nuclear materials

www.elsevier.com/locate/jnucmat

Current status of JAERI spallation target material program

K. Kikuchi *, T. Sasa, S. Ishikura [1], K. Mukugi [2], T. Kai, N. Ouchi, I. Ioka

Center for Neuron Science, Japan Atomic Energy Research Institute, Tokai-mura, Ibaraki-ken 319-1195, Japan
Mitsubishi Heavy Industry Ltd., Tokai-mura, Ibaraki-ken 319-1195, Japan

Abstract

In the joint project of spallation neutron source between JAERI and KEK, material technology has been developed for the mercury target in the neutron source facility, the lead–bismuth target in the transmutation test facility, superconducting accelerator, post-irradiation examination and the ion beam test. Design of target system is progressing for the mercury spallation target: a pressure test of moderator, an impacting test in mercury and a corrosion test have been carried out. For nuclear transmutation with ADS an engineering facility is proposed. A material corrosion test loop is built-up and SS316 and F82H steels are to be tested in a flowing Pb–Bi. Fracture toughness of superconducting cavity material was found to be considerably large at 4 K. Irradiated samples at SINQ are to be transported to JAERI Hot Laboratory. For simulating radiation damage small disk specimens were irradiated in single, dual and triple ion beam modes.

1. Introduction

There are two main programs going on in the neutron science project at JAERI under the framework of JAERI/KEK joint project [1]. They are neutron scattering research and research on accelerator-driven system (ADS) for nuclear transmutation. KEK also has proposed attractive research facilities. The major facilities which cover the whole program include a normal conducting proton linac, a superconducting proton linac, mercury spallation target for neutron scattering, 3 GeV synchrotron ring, 50 GeV synchrotron ring and ADS which consist of two test facilities, they are a critical assembly and a lead–bismuth target. Conceptual arrangement in the site of JAERI/TOKAI branch is shown in Fig. 1.

A new neutron source has planned to employ a basic science studies in structural biology, advanced material science, chemistry and experimental physics. In these fields, an intense proton accelerator is receiving attention as a potential supply of intense neutron beams as fission reactors cannot easily produce high neutron flux. The spallation reaction between target materials and a high-energy proton beam generates many neutrons and secondary particles. From neutronics considerations, the productivity of neutrons is favoured by the use of target materials as U, W, Ta, Hg and Pb, for example, because of their high density and high neutron yield, which result in a good neutron yield. There are two different types of target: solid and liquid metal targets. A megawatt spallation source is our final goal. Serious radiation damage and transient thermal stresses in the solid targets tend to favor the selection of a liquid target for larger power target. Solid target is an alternative option. Topics of materials research conducted in the spallation neutron source project are as follows:

Material in mercury spallation target;
Material for ADS target;
Material for superconducting cavity in proton linear accelerator;
PIE preparation for proton irradiation in STIP-I; and
Basic material research.

* Corresponding author. Tel.: +81-29 282 5058; fax: +81-29 282 6489.
E-mail address: kikuchi@popsvr.tokai.jaeri.go.jp (K. Kikuchi).
[1] On leave from Mitsubishi Heavy Industry Ltd., Tokai-mura, Ibaraki-ken 319-1195, Japan.
[2] On leave from Mitsubishi Electric Corporation, Tokai-mura, Ibaraki-ken 319-1195, Japan.

0022-3115/01/$ - see front matter
PII: S0022-3115(01)00498-6

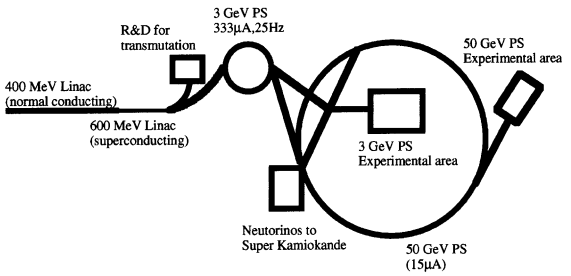

Fig. 1. Conceptual arrangement of accelerator and test facilities.

2. Material in mercury spallation target

2.1. Incident proton condition

Mercury target was selected as our design of megawatt neutron scattering facility in the following specification:

- The incident proton energy and current are 3 GeV and 333 μA, respectively, the total proton energy is 1 MW in short pulses at a frequency of 25 Hz.
- The duration of pulse width is about 1 μs and the reputation rate of pulses is approximately 40 ms.

As a consequence of short pulse, the deposit heat in the target, due to the spallation nuclear reactions that occur when energetic particles, for example, protons or neutrons, interact with a nucleus, leads to the production of pressure waves at the speed of sound in the target. In the mercury, it is estimated to be 1400 m/s when no bubbling occurs.

2.2. Target design

Fig. 2 shows the design view of spallation target [2]. Design works of mercury target have been doing in conjunction with neutronics, structural mechanics, fluid dynamics, heat transfer and safety. From the point of view of high neutron intensity, moderators favor to locate near target. So target shape is flattened and moderators will be put upon the top surface and beneath the bottom surface. Blade type flow distributor in the cross-flow target controls a mercury flow. Flow-guide plates also keep shape of target container. Target window will be a critical design part because of damage by proton–neutron irradiation, mercury corrosion and thermal stress cycling. It is emphasized that target container is to be replaced according to an operating schedule before a failure.

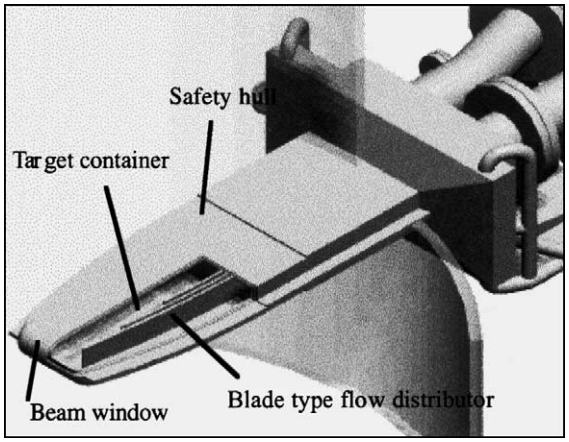

Fig. 2. Mercury spallation target [2].

Table 1 shows R&D items and related keywords for the mercury spallation target materials. In the mercury target and moderators design, a computer simulation is necessary to know the induced stress intensity and temperature as a function of time. ASTE collaboration work on the pressure wave measurement at BNL has played an important role to model a mechanical response of the target vessel [3]. The target fluid test demonstrated handling techniques of the liquid mercury. Burst test of moderator and impact test between mercury and structural alloys show fracture mode and material damage. Corrosion test in the liquid mercury shows a corrosion rate of the candidate materials. Irradiation damage under not only protons but also neutrons is a key issues for the life assessment of the target vessel.

2.3. Candidate materials

Candidate materials for the mercury target are type 316 stainless steel and F82H ferritic steel. These

Table 1
R&D items for mercury spallation target

R&D items	Technical keywords
Mercury target and moderators design	Modeling, design condition, candidate material, design criteria
Target fluid tests	Heat transfer, velocity, erosion
Burst test of moderator	Demonstration of modeling
Impacts tests interrupted between structrual material and mercury	Modeling, cavitation
Corrosion test in the mercury	Corrosion rate, candidate material
Irradiation damage	dpa, ductility

materials have the database of mechanical properties of post-irradiation examination under the proton and/or neutron. Design codes, which are used in nuclear fission reactor, are used as a design guide for the target engineering. A stress intensity value, S_m, is defined by yield stress σ_y and ultimate strength σ_u as shown in Eq. (1). It is nearly 200 MPa for SS316 austenitic stainless steel and 400 MPa for F82H ferritic steel, respectively. For short-pulsed spallation target a fatigue life is important. Allowable cycles to failure, N_d, is evaluated by Eqs. (2) and (3), here $\Delta\varepsilon_t$: total strain, N_f: number of cycles to failure, C_p, C_e, a_p, a_e: coefficients those are determined in the fatigue test, n: design cycles. Fatigue test results in the mercury environment were reported [4] but there was not a significant difference between mercury and air.

$$S_m = \text{Minimum}\left\{\frac{2}{3}\sigma_y, \frac{1}{3}\sigma_u\right\}, \tag{1}$$

$$\Delta\varepsilon_t = C_p N_f^{-a_p} + c_e N_f^{-a_e}, \tag{2}$$

$$\Sigma(n/N_d) < 1. \tag{3}$$

2.4. Design conditions

In the pulsed spallation target there are small changes of temperature corresponding to short pulses. But within seconds, a temperature in the mercury container becomes steady-state condition [5]. The container was cooled mainly by mercury. The maximum temperature of the target window is 170°C at the beam window and the minimum temperature of the window is 130°C in the engineering target design. Fig. 3 shows the target container deformed by the thermal stress. The target window is expanded by thermal elongation. The absolute displacement of target window is 0.025 mm maximally. The induced thermal stresses are 270 MPa. These results were obtained for the condition of 2.5 mm target window thickness, 1 MW design. The value of the proton power includes 30% safety margin; that is, the substantial proton power is 1.3 MW. Material used in the target design is the type 316 stainless steel. Further effort has been paid to 5 MW target design. This is a future direction.

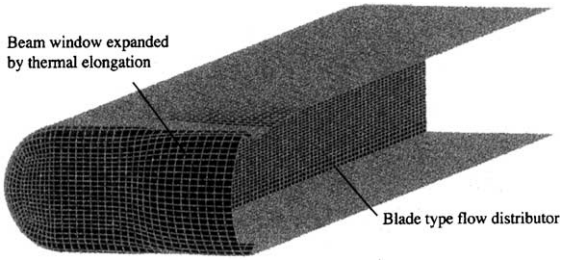

Fig. 3. Deformed target window due to thermal stress at a stationary operation; half model.

3. Material for lead–bismuth target

3.1. Concept of nuclear transmutation plant

Issues of R&D on ADS coupled with nuclear transmutation have been studied [1]. A conceptual design goal is shown in Fig. 4 [6]. The plant consists of Pb–Bi target equipped with beam duct in the center, fuel region, pump and steam generator. Fast neutrons produced in the spallation target will transmute long-lives nuclei to short-lives one in the fuel region surrounding the target. The lead–bismuth-cooled option is the primary candidate for the ADS. Lead–bismuth is the spallation target itself and also the coolant material of the primary system. It also offers the possibilities to achieve a harder neutron energy spectrum and to avoid a positive void reactivity coefficient. Its chemical inertness is particularly favorable for safety in the event of coolant leakage. But the disadvantage is a generation of reaction products such as Po and Hg. Again the technical issue for developing ADS, from points of views of engineering matters as the first step of development, is the beam window material. The beam window must endure against

- proton and neutron radiation damage;
- thermal stress cycling and
- corrosion–erosion.

3.2. ADS engineering test facility

In order to demonstrate ADS, the transmutation critical and engineering facilities have been designed conceptually. In the engineering test facility a lead–bismuth spallation target station is to be constructed. Fig. 5 illustrates a conceptual view of the engineering facility. An access cell is arranged behind a target station in order to prepare the post-irradiation examination (PIE). Objectives to build the facility are to demonstrate the material irradiation. The PIE will be done for development of materials available to ADS. Specification of the test facility is as follows:

- The incident proton energy and current are 600 MeV and 333 μA, respectively, the total proton energy is 200 kW in pulses at a frequency of 25 Hz.
- The duration of pulse width is about 500 μs and the period between pulses is approximately 40 ms.
- Average beam density is less than 30 μA/cm^2.
- Beam profile is 4 cm in diameter with the flat distribution.
- Target material is Pb–Bi alloy, 45%Pb–55%Bi.

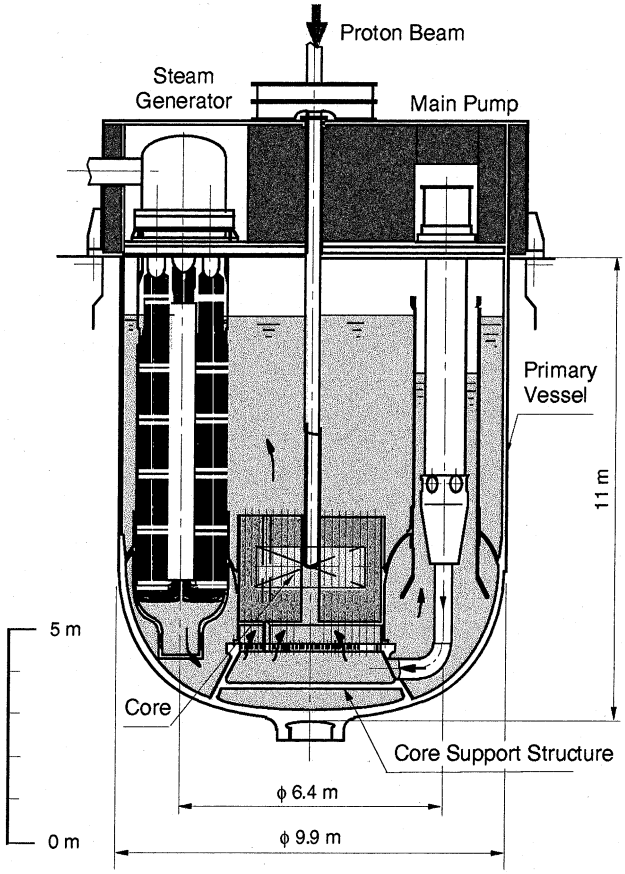

Fig. 4. Conceptual design of nuclear transmutation plant [6].

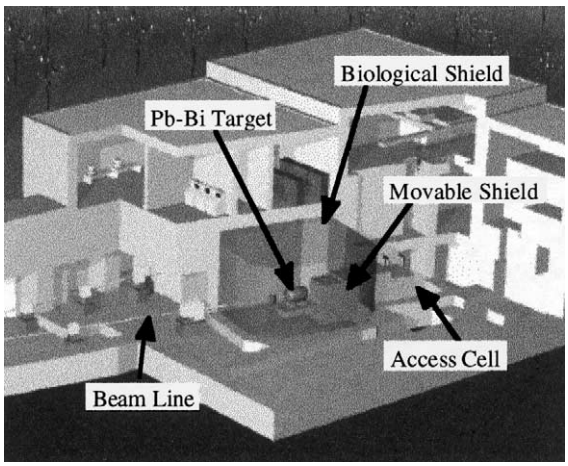

Fig. 5. Conceptual view of the engineering facility.

- Target temperature is 350°C/450°C (inlet/outlet).
- Target shape is a bullet type, 20 cm diameter × 60 cm length.

Pressure waves will not be a major technical issue, although it plays important roles in the mercury spallation target of 1 μs short pulse because a pulse width, 500 μs, is long enough to relax a temperature change rate.

There is a plan to install specimens in the flowing Pb–Bi. According to neutronics calculation done by ATRAS [7], the radiation damage of the type 316 stainless steel samples in the target will be over 10 dpa per year as shown in Fig. 6. ATRAS is an integrated code system to perform the neutronics analysis of ADS. It consists of NMTC/JAM [8,9] for high-energy particle transport, SCALE module for effective cross-section formation, TWODANT [10] for low-energy neutron transport and BURNER [11] for burnup calculation. The best sample for future ADS material development is the target window itself. It will be damaged 5 dpa per year under the Pb–Bi flow condition in the case study described above. Along the centerline the maximum dpa is over 10 but the gradient is very high. In this design, a beam profile is 4 cm in diameter with a flat distribution. Very high dpa area is located along a centerline within 3 cm diameter.

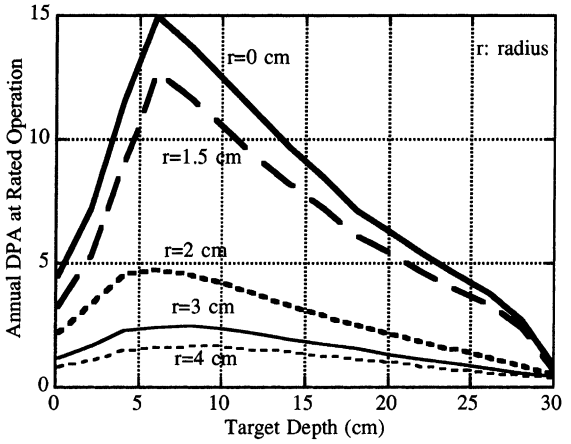

Fig. 6. Displacement per atom (dpa) of SS316 in the lead–bismuth target.

3.3. Liquid metal corrosion test

A lead–bismuth loop for material corrosion test is illustrated in Fig. 7. The test facility consists of test section, heater, cooler, electromagnetic pump, electromagnetic flow meter, surge tank and storage tank. The facility performances are as follows:

- Coolant: Pb–Bi (45–55%).
- Maximum Pb–Bi temperature: 450°C.
- Flow rate: 5000 cc/min.

Flow speed of Pb–Bi in the test section is one of the parameters. We expect around 1 m/s at the ADS target window. This test loop is constructed.There are three Pb–Bi test loops inclusive this one in Japan. The others exist in Central Research Institute of Electric Power Industry (CRIEPI) and Tokyo Institute Technology. The loop in CRIEPI was built to develop new steam generator with a direct contact heat transfer, under the condition of uncontrolled oxygen environment. They reported that modified 9Cr–1Mo and 2.25Cr–1Mo steels showed good evidence against corrosion at 500°C during 6000 h. On the contrary, type 304 stainless steel showed corrosive in the Pb–Bi [12]. First candidate material for our target container is the type 316 austenitic stainless steel. Alternative materials are F82H (8Cr–2W) ferritic steel [13], the oxide dispersion strengthened materials of ferritic steel and the high Cr/Fe steel [14]. In the corrosion tests an oxygen concentration in the lead–bismuth is to be controlled.Through the experiences in Institute of Physics and Power Engineering, it is recognized that the oxygen concentration must be within a particular range [15]. Low concentration will remove an oxide film from the material surface and high oxygen concentration makes lead oxide. It is important issue to find suitable values of oxygen concentration but a careful decision must be made if it is a right way to rely on the thin film on the material surface in order to protect materials from corrosive environment or not in the huge nuclear transmutation system.

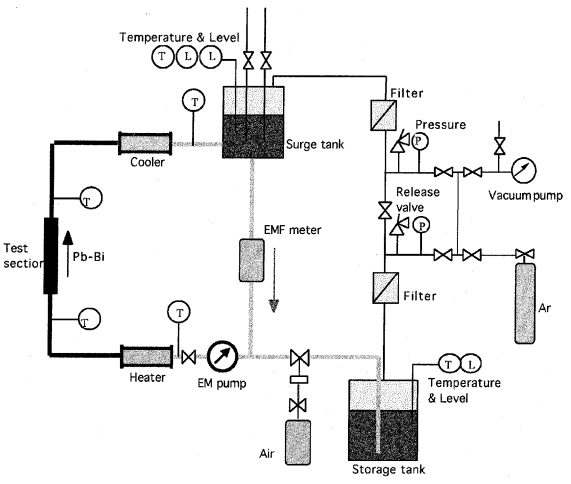

Fig. 7. Illustration of lead–bismuth corrosion test loop.

4. Material for superconducting cavity in proton linear accelerator

4.1. Cavity

High-intensity proton accelerators have been proposed with the superconducting proton linac. Superconducting cavities are arranged in pairs as shown in Fig. 8, each of which is enclosed in a helium vessel and suspended inside a vacuum jacket [16]. Pure niobium, Nb, is largely used in superconducting particle accelerators as sheet metal. Key issues in material technology to develop the sophisticated superconducting linac are structural material strength of

- Nb cavities,
- Nb – stainless steel and Nb–Ti joints

against the vacuum load and thermal stresses due to the joint of different materials in order to realize reduced $\beta = v/c$, particle velocity relative to the speed of light, and squeezed cavities. Typical results of fracture toughness tests of pure Nb plates of 3 mm thickness at the low temperature of 4 K are shown.

The commercially available pure Nb plates with high residual resistance ratio, RRR of over 2000 were supplied. High RRR value is an indication of good thermal conductivity. Table 2 shows the chemical composition of the material.

4.2. Fracture toughness test

Fracture toughness tests were performed at 4 K according to the ASTM E399-90. Specimens and other all

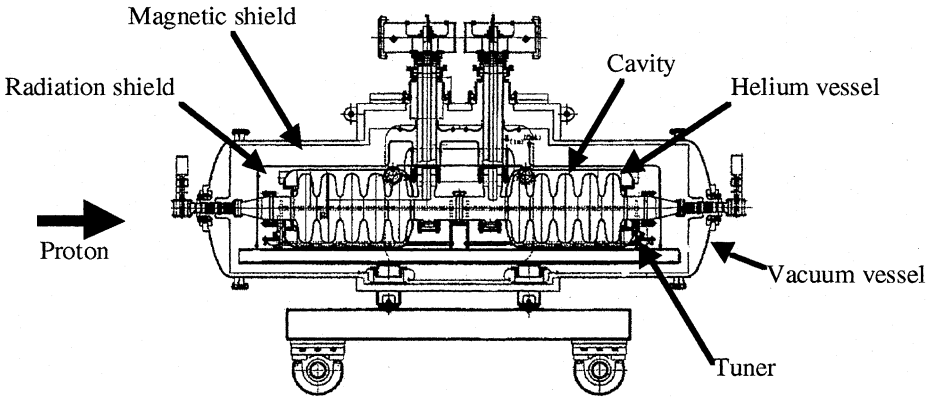

Fig. 8. A pair of the 600 MHz prototype 5-cell cavities ($\beta = 0.604$).

Table 2
Chemical composition of niobium plate

Element	H	O	N	C	Ta	Fe	Ti	W	Si	Mo	Zr	Nb
wt%	0.001 max	0.01	0.004	0.004	0.095	0.003	0.003	0.01 max	0.002	0.005 max	0.01 max	99.85 min

equipment were sunk in the liquid helium. Specimens were pulled at a speed of 0.12 mm/min, the crosshead speed. The clip gauge attached to the notch measured displacement of the specimens. Fig. 9 shows the photograph of the test. Table 3 summarizes the measured fracture toughness (K_Q), 95% secant load (P_Q) and crack length (a). K_Q is a tentative value of fracture toughness before evaluating a validity of the test. P_Q is a value of cross-point between a load–displacement curve and a line of 95% gradient. Fig. 10 shows the load–displacement curve of sample No.2 (bulk Nb), for example. Obtained fracture toughness of Nb was not valid for the plain–strain condition but is considerably large at 3 mm – thickness plate. Further R&D have been done for the numerical stress analyses and mechanical designs of cavities against the vacuum load, thermal stresses and so on were done in order to keep the stresses low sufficiently.

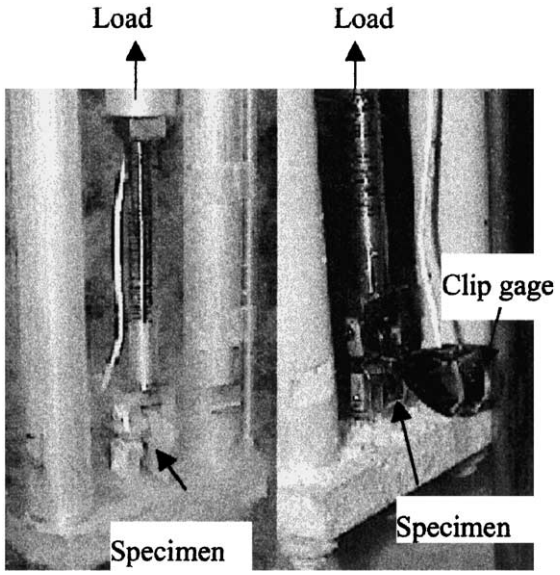

Fig. 9. Fracture toughness test at 4 K.

5. PIE preparation for proton irradiation in STIP-I

Post-irradiation experiment data under high-energy proton beam is necessary to evaluate a lifetime of the

Table 3
Fracture toughness K_Q of niobium plate in 3 mm thickness

No.	Condition	K_Q (MPa m$^{0.5}$)	Load P_Q (kN)	Crack length a (cm)
1	Nb TL	50.1	2680	1.206
2	Nb LT	45.5	2370	1.228
3	Weld bead	33.5	1720	1.240
4	Weld HAZ	35.0	1765	1.256

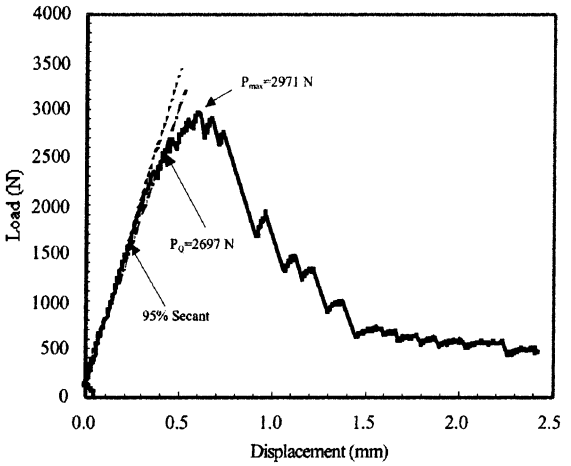

Fig. 10. Load displacement curve (No.2 Bulk Nb).

target container and/or the target window. Spallation target irradiation program (STIP) at SINQ has been progressing [17]. JAERI will share PIE for STIP-I materials, JPCA austenitic stainless steel and some of F82H ferritic steel. Tables 4 and 5 show chemical composition of these materials, respectively. Fig. 11 shows geometries of TEM disk, tensile specimens and bending fatigue specimens. We estimated the radioactivity of irradiated samples at SINQ using NMTC/JAM [9,10], MCNP/4A [18] and DCHAIN-SP [19]. The neutron and proton spectra were calculated using the NMTC/JAM and the MCNP/4A. The DCHAIN-SP calculates the decay and build-up of radioactivity using a neutron spectrum below 20 MeV and production yields induced by neutrons above 20 MeV and protons.

6. Basic materials research

A triple ion beam facility at JAERI was utilizable for simulating the effect of radiation on the mechanical properties, microstructure and corrosion resistance of

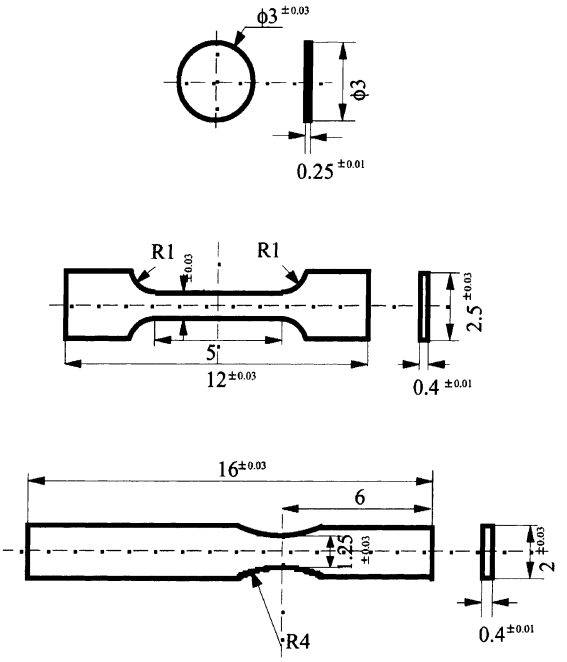

Fig. 11. PIE specimens for TEM disk(top), tension (middle) and ending (bottom).

the container materials under spallation conditions. A material tested is type 316 LN in the solution-annealed condition. The chemical composition is given in Table 6. The electrochemically polished disk specimens were irradiated in single, dual and triple (Ni^{3+}, He^{+}, H^{+}) ion beam modes at a temperature of 200°C.The irradiation condition was summarized in Table 7. The relationship between load and depth obtained by the nanoindentation test was expressed as the load/depth–depth curves, as shown in Fig. 12. The slope of the curve, denoted by S, is in direct proportion to the appearance hardness of the material. Moreover, it is well known that hardness can be related to yield strength. The ratios of S (irradiated) to S_0 (unirradiated) are shown in Fig. 13. It seems that implantation of Ni controls an increase in S.

Table 4
Chemical composition of JPCA (wt%)

Fe	Cr	Ni	Mo	Mn	Ti	Co	B	C	Si	P	S	N
Bal	14.14	15.87	2.29	1.54	0.22	0.028	0.004	0.058	0.50	0.026	0.004	0.003

Table 5
Chemical composition of F82H (wt%)

Fe	Cr	Ni	Mo	Mn	Ti	V	Nb	W	Ta	Cu	C	Si	P	S	N
Bal	7.87	0.02	0.003	0.1	0.004	0.19	0.0002	1.98	0.03	0.01	0.09	0.07	0.003	0.001	0.007

Table 6
Chemical composition of type 316LN

Fe	C	Si	Mn	P	S	Ni	Cr	Mo	O	N
Bal	0.019	0.6	0.82	0.027	0.001	12.23	17.70	2.15	0.002	0.06

Table 7
Irradiation condition for type 316LN

	Dose (dpa)	He (appm)	H (appm)
Ni	13.1	0	0
Ni, He, H	11.5	2344	17 705
Ni, He	11.2	2748	0
He, H	0.1	1533	16 440
Ni	10.6	0	0
Ni, He	11.13	1468	0

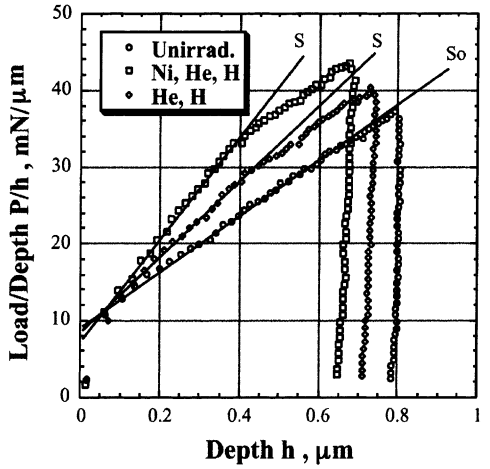

Fig. 12. Load/depth vs. depth curve.

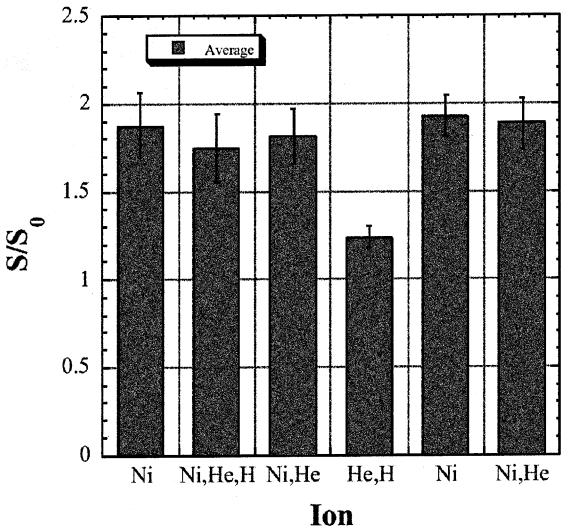

Fig. 13. Change of slopes by irradiation.

7. Summary

Material technology related to high-intensity proton accelerator project, which covers the field of neutron scattering, accelerator-driven system, superconducting proton accelerator, post-irradiation examination and basic research was introduced. International cooperative works have been done for material experiment in STIP and MEGAPIE, ASTE collaboration at BNL and mercury target collaboration with ORNL.

Acknowledgements

We thank the joint project team of JAERI and KEK for a support of this work.

References

[1] The joint project for high-intensity proton accelerators, JAERI-Tech 99–056, 1999.
[2] R. Hino, M. Kaminaga, K. Haga, T. Aso, H. Kinoshita, H. Kogawa, S. Ishikura, A. Terada, K. Kobayashi, J. Adachi, T. Teraoku, K. Takahashi, S. Honmura, S. Sasaki, Present status of spallation target development – JAERI/KEK joint project – ICANSXV, Tsukuba, 2000.
[3] M. Futakawa, K. Kikuchi, H. Conrad, H. Stechemesser, Nucl. Instrum. Meth. Phys. A 439 (2000) 1.
[4] S.J. Pawel, J.R. Distefano, J.P. Strizak, C.O. Stevens, E.T. Manneschmidt, Screening Test Results of Fatigue Properties of Type 316LN Stainless Steel in Mercury, ORNL/TM-13759, SNS/TSR-0097, 1999.
[5] K. Kikuchi, in: OECD Proceedings of WS on Utilization and Reliability of High-Power Proton Acelerators, Japan, 1998, 381–388.
[6] H. Takano, K. Nishihara, K. Tsujimoto, T. Sasa, H. Oigawa, K. Kikuchi, Y. Ikeda, T. Takizuka, T. Osugi, in: Proceedings of the OECD NEA P&T IEM3, 2000.
[7] T. Sasa et al., Accelerator-driven transmutation reactor analysis code system-ATRAS-, JAERI-Data/code 99-007, 1999.
[8] K. Niita et al., Analysis of the proton-induced reactions at 150 MeV–24 GeV by high-energy nuclear reaction code JAM, JAERI-Tech 99-065, 1999, (Japanese).
[9] H. Takada, Recent progress of nucleon–meson transport code development at JAERI, Proceedings of the International Conference on Mathematics and Computation, Reactor Physics and Environmental Analysis in Nuclear Applications, September 27–30, 1999, Madrid, Spain, 2000.

[10] R.E. Alcouffe et al., Users Guide for TWODANT: A Code Package for Two-Dimensional, Diffusion-Accelerated, Neutral-Particle Transport, LA-10049-M, 1990.
[11] D.R. Vondy, G.W. Cunningham, Exposure Calculation Code Module for Reactor Core Analysis: BURNER, ORNL-5180, 1979.
[12] I. Kinoshita, A. Ohto, Y. Nishi, System concept and fundamental heat transfer characteristics of direct contact high-reliable SG for FBRs, CRIEPI Report T92024, 1993 (Japanese).
[13] M. Tamura, H. Hayakawa, M. Tanimura, A. Hishinuma, T. Kondo, J. Nucl. Mater. (1986) 1067.
[14] A. Hishinuma et al., Solid State Phys. (2001) (to be printed).
[15] R.B. Gromov, Yu.I. Orlov, P.N. Martynov, K.D. Ivanov,V.A. Gulevsky, in: H.U. Borgstedt (Ed.), Liquid Metal Systems, Plenum, New York, 1995.
[16] K. Mukugi, N. Ouchi, K. Ishio, Y. Tsuchiya, K. Kikuchi, A. Naito, K. Saito, J. Kusano, M. Mizumoto, in: Proceedings of the Ninth Workshop on RF-Superconductivity, Santa Fe, 1999 (to be published).
[17] Y. Dai, SINQ Irradiation Experiment Report, PSI report TM-36-98-11, 1998.
[18] J.H. Briesmeister (Ed.), MCNP – A General Monte Carlo N – Particle Transport Code, Version 4A, La-12625, 1993.
[19] H. Takada, Development of the D CHAIN-SP code for Analyzing decay and build-up characteristics of spallation products, JAERI-Data/Code 99-008, 1999.